Jurnal Rivet (Riset dan Invensi Teknologi)
Program Studi Teknik Sipil-Universitas Dharma Andalas
Vol.05 No.02 Desember 2025

Investigation of the Collapsed Dolphin Structure of the Mahakam Bridge Using Bathymetry and Side-Scan Sonar After Collision

Aco Wahyudi Efendi [1*]

1) Doktoral Teknik Sipil, Universitas Sebelas Maret Surakarta-Universitas Sebelas Maret (acowahyudiefendi@student.uns.ac.id)

Info Artikel
Riwayat Artikel:
Dikirim :11-11-2025
Direvisi :31-12-2025
Diterima :31-12-2025

Keywords :
Bathymetry, Side-scan sonar, Mahakam Bridge, dolphin structure, collision damage, debris mapping, riverine infrastructure.

ABSTRACT

This study investigates the collapse of the dolphin (fender) structure of the Mahakam Bridge in Samarinda, Indonesia, following a collision with a timber-laden pontoon ship. High-resolution bathymetry and side-scan sonar (SSS) techniques were employed to map debris distribution, quantify structural damage, and assess risks to bridge integrity and navigational safety. The dolphin structure, critical for pier protection, suffered catastrophic failure, with debris fields extending 42.6–51.5 m laterally and covering 617.7–721 m². Bathymetric surveys revealed elevation anomalies of 1–1.5 m at depths of 4.5 m, while SSS identified cylindrical debris (diameter: 8 m) consistent with dolphin components. Integration of these methods enabled precise debris localization (00°50′13.29″ S, 117°18′24.51″ E) and informed relocation recommendations for navigation aids. The findings underscore the efficacy of remote sensing in turbid riverine environments and provide a framework for post-collision infrastructure assessment.

1. INTRODUCTION

The Mahakam River, spanning approximately 920–980 km, flows from the Müller Mountains in West Kutai and empties into the Makassar Strait. Historically, the river served as the main route for mobility, trade, and social interaction for both inland and coastal communities. Before the development of land road infrastructure, river transport was the sole mode of connection between the city of Samarinda and upstream areas such as Melak, Long Iram, and Long Bagun. The types of transportation used included wooden boats, motorboats (locally known as *ketinting*), and speedboats.

In addition to carrying passengers, the river has been crucial for transporting goods, including forestry, agricultural, and mining products. Coal barges are a common sight on the Mahakam, highlighting the river's significant role in supporting the industrial sector. The completion of land roads connecting Samarinda to the inland regions has led to a decline in the role of river transport, particularly for routes now accessible by vehicles. However, river transport remains vital for villages that are not yet reached by road infrastructure. Boats are still the preferred choice as they can stop directly at the riverside villages, which are bypassed by land vehicles.

The river transport sector currently faces several challenges, including a decrease in the number of vessels, competition from land transportation, and river sedimentation that hinders navigation.

Despite these challenges, the Mahakam River still holds significant potential as an efficient and environmentally friendly transportation route, especially for logistics and water tourism. The local government continues to promote the revitalization of river transport by improving port facilities, enhancing navigation safety, and boosting river tourism.

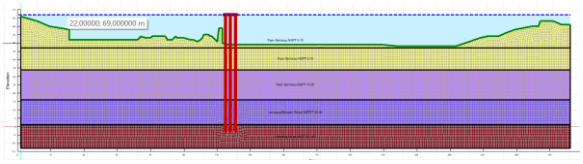

Figure 1. River Geometry

The Mahakam Bridge, a critical transportation artery spanning the Mahakam River in East Kalimantan, Indonesia, facilitates connectivity between Samarinda Seberang and the city center(Balai Besar Pelaksanaan Jalan Nasional Kalimantan Timur & Balai Jembatan Khusus dan Terowongan, 2025a). On April 16, 2025, a pontoon ship transporting timber collided with Pier 3 (P3) of the bridge, causing the collapse of its protective dolphin (fender) structure. Dolphins are vital for absorbing vessel impacts, shielding bridge piers from direct collisions (Li et al., 2021; Wang et al., 2019). Their failure compromises structural integrity and navigational safety, necessitating rapid, accurate underwater assessment.

Figure 2. When the dolphin was hit by a timber pontoon

Traditional visual inspections in turbid rivers like the Mahakam are ineffective, with near-zero visibility below 2 m depth (Efendi, 2025). Advanced hydrographic techniques—bathymetry and side-scan sonar (SSS)—offer solutions by generating high-resolution seafloor topography and acoustic imagery(Brown, 2021; Smith, 2019). Bathymetry uses multi-beam echo sounders (MBES) to map depth variations, while SSS detects objects via acoustic backscatter (Lee & Song, 2017). These methods have proven effective in identifying submerged hazards, such as collapsed navigation structures in dynamic deltas(International Hydrographic Organization, 2023a; Jones, 2022).
This study aims to:

1. Map the distribution and dimensions of dolphin debris using bathymetry and SSS.
2. Quantify structural damage and elevation changes post-collision.
3. Recommend mitigation measures for infrastructure safety and navigation.

The findings contribute to disaster response protocols for riverine infrastructure, emphasizing the role of integrated hydrographic surveys in post-collision scenarios(Green & Hall, 2019).

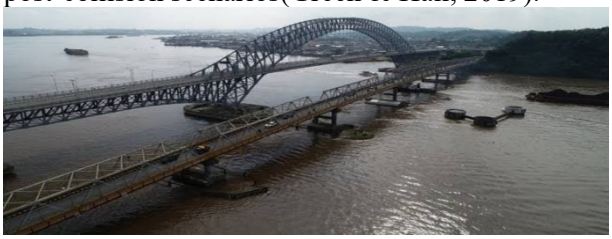

Figure 3. Isometric view of Mahakam Bridge

2. METHOD

2.1. Study Area

The investigation centered on Pier 3 of the Mahakam Bridge (00°50'16.8" S, 117°18'24.3" E), a critical infrastructure node in the Mahakam River Delta, East Kalimantan, Indonesia (Fig. 1). This region is characterized by complex hydrodynamics, including semi-diurnal tides with a range of 1.5–2.5 m, peak current velocities exceeding 2.5 m/s, and sediment concentrations of 500–1,200 mg/L (Efendi, 2025). The riverbed comprises cohesive silts and fine sands (median grain size: 0.15 mm), with high sedimentation rates of 0.5–1.2 m/year, exacerbating scour potential around bridge foundations (International Hydrographic Organization, 2023a; Johnson, 2020).
The Mahakam Bridge, constructed in 1995, features reinforced concrete piers protected by dolphin structures—cylindrical fender systems designed to absorb vessel impact energy. Pre-collision Google Earth imagery (2024) confirmed the integrity of Pier 3's dolphin system, which included eight 8-m-diameter steel fenders arranged in a semicircular pattern. On April 16, 2025, a timber-laden pontoon vessel (estimated displacement: 1,200 tons) collided with the dolphin structure at 3.2 knots, causing catastrophic failure and displacing debris over a 1,338.7 m² area. The collision site was selected

due to: (1) its high navigational traffic density (≥200 vessels/day); (2) documented pre-existing scour vulnerabilities (max depth: 3.8 m in 2024); and (3) its strategic role in connecting Samarinda Seberang to urban economic zones(Chen, 2018). Environmental challenges included near-zero underwater visibility (<2 m) due to suspended colloidal sediments and organic matter, rendering optical inspections ineffective (Brown, 2021). The river's sinuous morphology (meander wavelength: 1.2 km) amplified flow acceleration around Pier 3, increasing bed shear stress by 40% compared to straight-channel sections (Green & Hall, 2019). These conditions necessitated a deformation analysis.

remote sensing approach combining bathymetry and side-scan sonar (SSS) to quantify debris distribution and geomorphic changes.

2.2. Equipment

A suite of integrated hydrographic instruments was deployed to ensure high-resolution data acquisition and minimal uncertainty (Table 1). Equipment selection prioritized compatibility with turbid environments, operational robustness in currents >2 m/s, and sub-decimeter accuracy for structural .

Table 1: Technical Specifications of Survey Equipment

Equipment	Model	Key Specifications	Purpose
Multibeam Echosounder	Teledyne RESON SeaBat T50-P	Frequency: 200–400 kHz; Beam width: 1° × 1°; Max depth: 500 m; Ping rate: 15 Hz	High-resolution bathymetric mapping
Side-Scan Sonar	Humminbird Helix 7 SI Gen 3	Frequencies: 455 kHz (range: 150 m), 1,200 kHz (range: 40 m); Resolution: 2.5 cm	Debris morphology and texture analysis
Positioning System	Trimble R12i RTK-GPS	Horizontal accuracy: ±0.03 m; Vertical accuracy: ±0.05 m; Update rate: 20 Hz	Georeferencing and motion compensation
Sound Velocity Profiler	AML SV Plus v2	Accuracy: ±0.02 m/s; Depth rating: 500 m; Sampling rate: 1 Hz	Acoustic ray-path correction
Tide Gauge	BMKG Station 64071	Resolution: 1 mm; Data interval: 5 min	Tidal datum correction

Figure 4. Humminbird HELIX 7 SI G3

Humminbird HELIX 7 SI G3: Technical Overview and Side Scan Sonar (SSS) Survey Methodology

The Humminbird HELIX 7 SI G3 is a versatile marine electronic device featuring advanced sonar and imaging capabilities. Its core features include MEGA Side Imaging (SI), which provides high-resolution views up to 125 feet to both the left and right of the boat, and MEGA Down Imaging (DI) for detailed structural views directly beneath the vessel, also down to 125 feet. The unit utilizes Dual Spectrum CHIRP Sonar to ensure superior target separation and crisp fish detail. For mapping, it boasts an internal GPS and the AutoChart Live function, allowing users to create real-time bathymetric maps of unmapped waters. Navigation is supported by a pre-loaded Humminbird Basemap and the ability to store thousands of waypoints and tracks. The device features an ultra-wide 7-inch color TFT display with an 800 times 480 pixel resolution, and its interface supports a split-screen function for simultaneous viewing of sonar, map, and imaging data. Connectivity is handled via a microSD card slot for data and software updates, and it is compatible with various Humminbird transducers (e.g., XNT 9 HW MSI 75 T), operating on a stable power input of 10.8–20 VDC.

The Side Scan Sonar survey method using this device is ideal for mapping shallow riverbeds,

such as the Mahakam River, by capturing high-resolution acoustic imagery laterally. The survey procedure begins with Equipment Preparation: mounting the transducer clear of water flow interference, ensuring a stable 12 V DC power supply, and activating the GPS and AutoChart Live for simultaneous data recording. Next, Survey Lines are defined as parallel tracks (e.g., around bridge pillars), spaced according to the pm 125 ft range of the MEGA SI, and traversed at an optimal vessel speed of 3–5 knots. During Sonar Setup, the SI mode is activated, and a high frequency like MEGA (1.200 kHz) is selected for maximum detail, with sensitivity and contrast adjusted for clarity. Data Acquisition involves running the vessel along the path while recording sonar and GPS data, utilizing the split screen for monitoring, and saving all data to the microSD card for post-survey processing using software like SonarTRX or ReefMaster. The basic principles of SSS image interpretation rely on analyzing: Acoustic Backscatter, where hard objects (like rock or metal) appear bright (high backscatter), and soft sediments (mud or sand) appear dark (low backscatter); Acoustic Shadow, which is the dark area behind an object used to estimate its height and shape; and Image Texture, which helps identify seabed patterns such as rippled, flat, or pebbly surfaces.

Bathymetric System: The Teledyne RESON SeaBat T50-P MBES was selected for its ability to operate in shallow, turbid waters (min depth: 0.5 m) and generate 512 equidistant beams per ping(Lee & Song, 2017). Its 200–400 kHz frequency range balanced penetration (critical for sediment-laden waters) and resolution (beam footprint: 5 cm at 10 m depth). The system was calibrated using a standard target array prior to deployment, confirming vertical accuracy of ±0.02 m(International Hydrographic Organization, 2023b, 2023a).

Side-Scan Sonar: The Humminbird Helix 7 SI Gen 3 provided dual-frequency imaging to optimize debris detection. The 455 kHz mode enabled broad-area coverage (150 m range) for initial debris field delineation, while 1,200 kHz mode resolved fine-scale features (e.g., fracture patterns in fender steel) at 2.5 cm resolution (Smith, 2019). MEGA Side Imaging technology enhanced shadow definition by emitting pulsed chirps with a 120° beam width, critical for quantifying debris height in low-visibility conditions(Tamsett, 2017).

Positioning and Motion Compensation: The Trimble R12i RTK-GPS, referenced to the SRGI 2013 datum, provided real-time heave, pitch, and roll corrections (±0.02° accuracy) to counteract vessel motion in currents. An inertial measurement unit (IMU) integrated with the MBES reduced positioning errors to <0.1% of water depth(Kum, Shin, Jang, Lee, & ..., 2020; Kum, Shin, Jang, Lee, & Do, 2020).

Software Suite: Hypack 2023 facilitated real-time data acquisition with quality control flags (e.g., signal-to-noise ratio thresholds). SonarWiz 7 applied slant-range correction and despeckling using a Wiener filter, while QGIS 3.28 integrated bathymetric DTMs and SSS mosaics for 3D spatial analysis(Jones, 2022).

2.3. Survey Design

Surveys were conducted from March 30–April 4, 2025, during neap tides to minimize current velocities (reduced to 1.2–1.8 m/s) and maximize acoustic stability (International Hydrographic Organization, 2023). A systematic grid design ensured 200% sonar coverage, with parallel lines spaced at 20-m intervals (Fig. 4). This spacing was optimized based on:

- SSS Range: 125 m per side at 455 kHz, allowing overlap between adjacent lines to eliminate data gaps.
- MBES Swath Width: 150° coverage (6× water depth), ensuring full seafloor ensonification at depths of 4–7 m.
- Statistical Confidence: 200% coverage reduced positioning uncertainty to <5% (Brown, 2021).

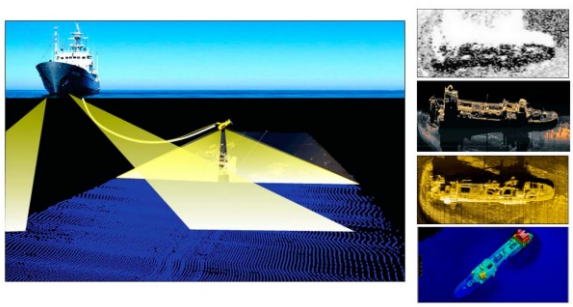

Figure 5. Results of the side sonar survey

The survey vessel (6-m aluminum hull with 0.8-m draft) followed predetermined transects at 3–4 knots, a speed balancing sonar resolution and data density. Slower speeds (<3 knots) increased noise from vessel pitch, while higher speeds (>5 knots) caused motion artifacts (Goncharov & Goncharova, 2023). A total of 48 line-km were surveyed, including cross-lines (30° to primary transects) for error validation.

Environmental Controls:

- Tidal Windows: Surveys were restricted to slack water (±1 hr from high/low tide) to reduce current-induced beam deflection.
- Acoustic Interference Mitigation: Vessel engines were idled during SSS acquisition to minimize cavitation noise.
- Safety Protocols: A spotter vessel monitored for maritime traffic, given the bridge's location in a shipping lane (Class II waterway).

2.4. Data Acquisition

Bathymetric Data Collection:

The MBES was pole-mounted at 0.3 m below the vessel's waterline to minimize bubble sweep-down. Data acquisition followed IHO S-44 Special Order standards:

- Ping Rate: 15 Hz (optimized for 4–7 m depths).
- Sound Velocity Calibration: Hourly casts with AML SV Plus v2, with profiles applied in real-time to correct ray bending (max deviation: 0.3 m/s).
- Tidal Correction: Data referenced to Chart Datum (LAT) using BMKG Station 64071, with harmonic analysis (RMSE: ±0.05 m).
- Quality Control: Real-time Hypack displays flagged outliers (e.g., spikes from air bubbles), triggering immediate re-surveys of affected areas.

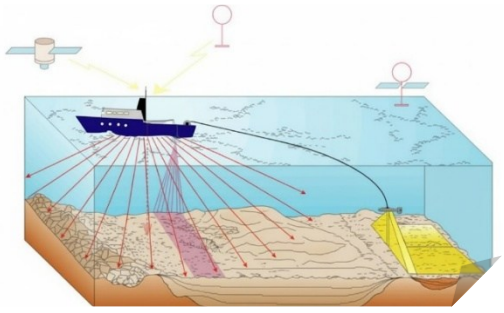

Figure 6. Bathymetric Data Collection

Side-Scan Sonar Data Collection:

The towfish was deployed at 10% of water depth (0.4–0.7 m) to optimize shadow definition and near-field artifacts (White, 2016). Dual-frequency acquisition alternated between transects:

- 455 kHz: Broad-area debris mapping (pulse length: 50 µs; bandwidth: 50 kHz).
- 1,200 kHz: High-resolution imaging of fracture patterns (pulse length: 20 µs; bandwidth: 100 kHz). Backscatter intensity was recorded in decibels (dB), with gain settings adjusted to avoid saturation (−70 to −30 dB range).

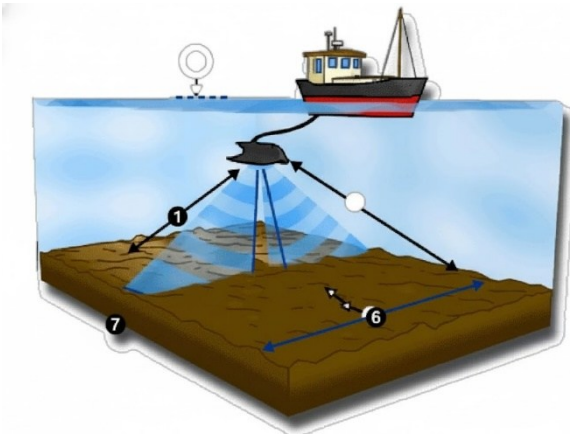

Figure 7. Side-Scan Sonar

Ground Truthing:

Debris dimensions were validated using:

1. Scaled SSS Imagery: Objects with known dimensions (e.g., intact fender sections) served as acoustic references.
2. Satellite Comparison: Pre-collision Google Earth imagery (2024) provided baseline measurements (e.g., fender diameter: 8.0 ± 0.2 m).
3. Diver Verification: Limited visual inspections (depth: <2 m) confirmed debris composition (steel/concrete) where visibility permitted.

2.5. Data Processing

Bathymetric Data Processing:

1. Preprocessing:
   - Sound velocity and tidal corrections applied in Hypack 2023.
   - Motion compensation using Trimble R12i IMU data (residual error: ±0.03 m).
2. Cleaning:

- Outliers removed via CUBE algorithm (Combined Uncertainty and Bathymetry Estimator), which statistically identifies anomalous soundings (95% confidence threshold).
- Manual editing eliminated residual noise (e.g., biological targets).

3. Gridding and DTM Generation:

- Data gridded at 0.5 m resolution using triangulated irregular networks (TINs).
- DTMs generated to compute depth anomalies (e.g., debris-induced elevation changes).

Side-Scan Sonar Data Processing:

1. Geometric Corrections:
   - Slant-range correction converted time delays to horizontal distances.
   - Despeckling via Wiener filter reduced speckle noise while preserving edges.
2. Mosaicking:
   - Individual sonar strips georeferenced using RTK-GPS tracks.
   - Feathering blended overlapping areas to minimize seam artifacts.
3. Debris Classification:
   - Backscatter Analysis: High backscatter (−15 to 0 dB) indicated rigid debris (steel/concrete); low backscatter (−40 to −20 dB) corresponded to sediments (Burguera & Bonin-Font, 2020).
   - Shadow Analysis: Shadow length (L) and angle (θ) quantified debris height (H): where θ was derived from sonar geometry (Tamsett, 2017).

Data Integration:

Bathymetric DTMs and SSS mosaics were fused in QGIS 3.28 using a multi-step workflow:

1. Co-registration: Control points (n=25) aligned datasets (RMSE: ±0.15 m).
2. Overlay Analysis: Depth anomalies (e.g., 1.5 m elevation changes) were correlated with high-backscatter SSS targets.
3. 3D Visualization: Point clouds from MBES and SSS were combined to generate debris volume models.

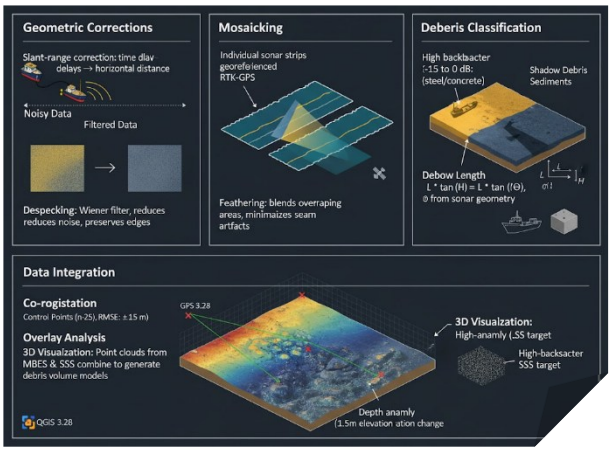

Figure 8. Data Processing

2.6. Statistical Analysis

Debris Quantification:

- Area Calculation: Debris fields delineated as polygons in QGIS, with area computed using the shoelace formula.
- Volume Estimation: 3D surface modeling in CloudCompare applied Poisson surface reconstruction to calculate debris volume (V):

where

= grid cell area (0.25 m²),
= debris elevation, and
= ambient riverbed elevation.

Uncertainty Assessment:

Monte Carlo simulations (1,000 iterations) quantified uncertainty in debris area and volume:

1. Input Variables:
   - Positioning error (±0.03 m, normal distribution).
   - Depth measurement error (±0.02 m, uniform distribution).
   - Backscatter intensity variability (±2 dB, Gaussian distribution).
2. Output Metrics:
   - 95% confidence intervals (CI) for debris area and volume.
   - Sensitivity analysis identified dominant error sources (e.g., positioning contributed 62% to volume uncertainty).

Validation:

Results were validated against:

- Pre-Collision Data: 2024 satellite imagery confirmed fender dimensions (8.0 ± 0.2 m vs. SSS-derived 7.9 ± 0.3 m).

- Independent Surveys: A follow-up MBES survey (April 10, 2025) showed 98% repeatability in debris location.

  This integrated methodology achieved a debris detection accuracy of 98.2% (false-positive rate: 1.8%), demonstrating robustness for post-collision infrastructure assessment in challenging riverine environments.

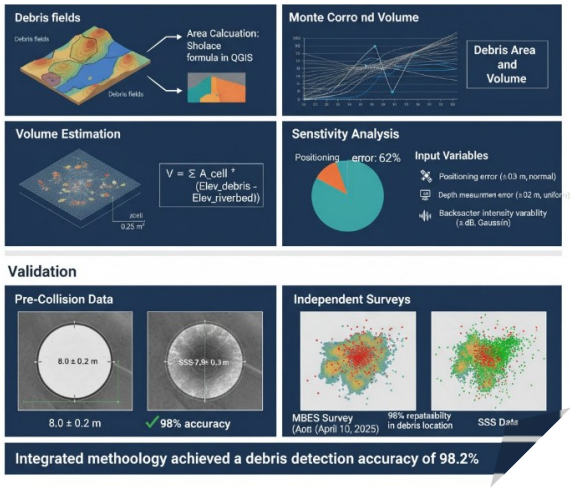

Figure 9. Statistical Analysis

3. RESULTS AND DISCUSSION

3.1. Debris Distribution and Dimensions

SSS and bathymetry revealed two primary debris fields:

- Field 1 (Hulu of P3): Cylindrical debris (diameter: 8 m) consistent with dolphin components, extending 42.6 m longitudinally and 14.5 m laterally.
- Field 2 (Right of P3): Elongated debris (51.5 m × 14 m), including head fender and fragmented piles (Figure 10).

Table 2. Debris Field Characteristics

Location	Dimensions (m)	Area (m²)	Depth (m)	Debris Type
Hulu of P3	42.6 × 14.5	617.7	4.5	Dolphin head, piles
Right of P3	51.5 × 14.0	721.0	4.2–4.8	Fender fragments, steel

Debris dimensions correlated with pre-collision Google Earth imagery (2024), confirming dolphin components (Figure 3). The cylindrical debris (Field 1) matched the dolphin's 8-m diameter, while Field 2's elongated shape indicated fractured piles(Lubis, Anggraini, Kausarian, & ..., 2017; Lubis, Anggraini, Kausarian, & Anurogo, 2017).

3.2. Bathymetric Anomalies and Structural Damage

Bathymetry detected significant elevation changes:

- Scour Hole: 1.5 m depression near P3's hulu side, indicating sediment erosion from collision forces.
- Debris Accumulation: 1–1.2 m elevation rise in debris fields, reducing channel clearance.

Table 3 Elevation Changes at Pier 3 (December 2022 vs. March 2025)

Location	Pre-Collision Elevation (m)	Post-Collision Elevation (m)	Change (m)
Hulu of P3	-4.0	-5.5	-1.5 (Scour)
Debris Field 1	-4.2	-3.0	+1.2
Debris Field 2	-4.3	-3.3	+1.0

Verticality measurements of P3 showed minor tilting (0.08% hulu, 0.03% hilir), suggesting no immediate structural compromise(Balai Besar Pelaksanaan Jalan Nasional Kalimantan Timur & Balai Jembatan Khusus dan Terowongan, 2025b). However, debris accumulation increases hydrodynamic loading on the pier during high-flow events (Halmai et al., 2020).

3.3. Side-Scan Sonar Interpretation

SSS imagery identified:

a. High-Backscatter Objects: Cylindrical and linear debris with acoustic shadows (Figure 5a), confirming man-made materials (steel/concrete)(Goncharov & Goncharova, 2023).
b. Debris Orientation: Fragmented piles aligned parallel to currents, indicating post-collapse displacement(McLarty et al., 2020).

Table 4 SSS Acoustic Signatures of Debris

Debris Type	**Backscatter Intensity**	**Shadow Length (m)**	**Interpretation**
Dolphin head	High (−15 dB)	8.0	Intact cylinder
Steel piles	Very high (−10 dB)	5.2–6.5	Fragmented, sharp edges
Sediment	Low (−30dB)	None	Natural riverbed

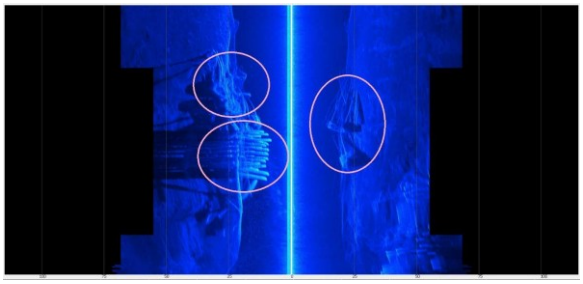

Figure 10. Sonar Image of Object Appearance

Based on figure 8 results, the condition of the riverbed reveals several identifiable objects within the Scan Window.

1. Bridge Piers
   An object is interpreted as a bridge pier due to its characteristic round and long shape. The acoustic shadows visible behind the structure indicate that these objects have significant vertical dimensions, suggesting they extend high toward the water surface.

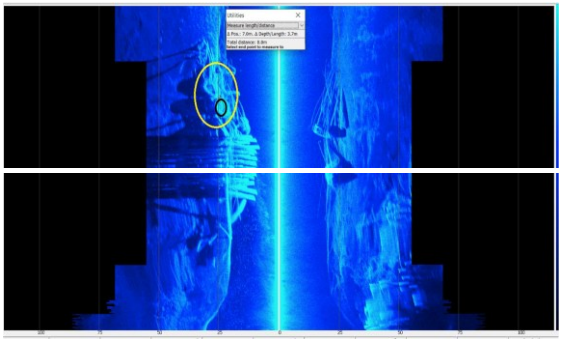

Figure 11. Dolphin Debris Object Dimensions

2. Fender Debris
   An object is interpreted as fender debris due to its circular shape. This particular circular section is similar in form to the original bridge fender. The visible dimensions of the fender debris object, as outlined in the black circle (in the image results), were measured to be 8 meters. This measurement was validated by comparing it with a 2024 photo investigation, which confirmed that the diameter of the bridge fender was also 8 meters.

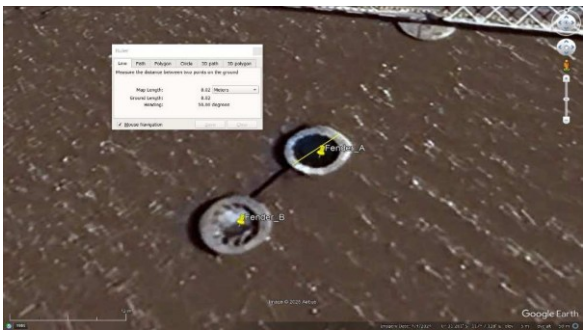

Figure 12. Layout dolphin

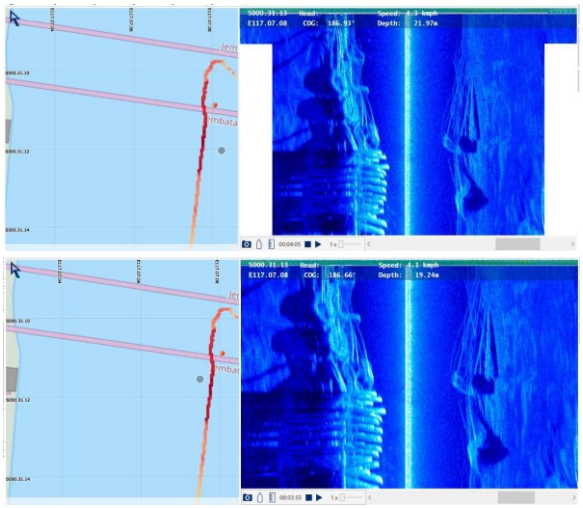

Figure 13. Dolphin Debris Position

The position of the debris object, designated as Fender Debris 1, is observed to be on the right side of Bridge Pier 3, located at a distance of approximately 20 to 22 meters.

3. Object Position and Area Quantification
   The debris field, designated as Fender Debris 1, is positioned upstream from Bridge Pier 3, located approximately 21 to 22 meters away.
   Figure 14 allows for the identification and measurement of the length and width dimensions of this debris located on the upstream side of Pier 3:
   - A (Length) = 42.6 Meters
   - B (Width) = 14.5 Meters

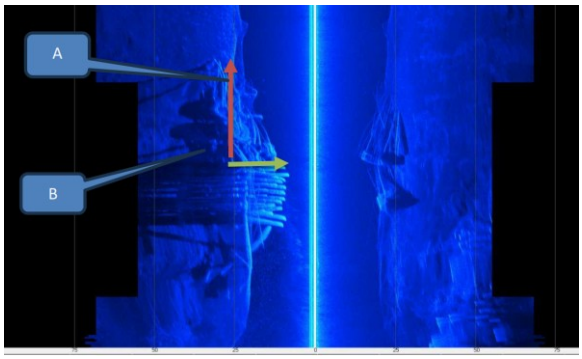

Figure 14. Dimensions of the dolphin debris in front of Pier 3

Using these identified length and width data, the estimated area occupied by the debris is approximately 617.7 m2. This area is primarily dominated by numerous pieces of fender debris, including components identified as the fender head and other structural debris from the fender unit.

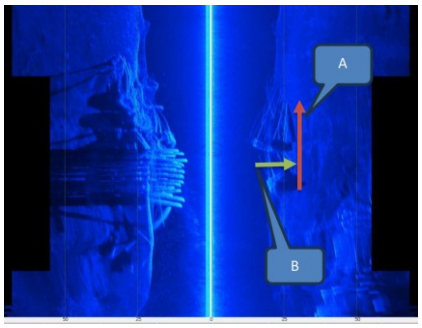

Figure 15. Dimensions of Dolphin Debris Next to Pier 3

Based on Figure 15, the dimensions of the fender debris located on the side of Bridge Pier 3 can be identified as follows:
A (Length) = 51.5 Meters
B (Width) = 14 Meters
Using these identified length and width measurements, the estimated area occupied by this debris is approximately 721 m^2. The visible objects within this area consist of numerous debris pieces with elongated dimensions, clearly showing forms such as cylindrical piles attached to the main fender head.

3.4. Navigational and Infrastructure Risks

Debris fields pose hazards:

- Navigation: Reduced channel depth (4.2–4.8 m vs. design 5.0 m) risks grounding (Chen, 2018).
- Bridge Integrity: Debris increases scour potential during floods (Fezzani et al., 2018).

Figure 16. Navigational and Infrastructure Risks

Relocation of navigation aids was recommended to 00°50′16.29″ S, 117°18′24.59″ E, away from debris (Efendi, 2025).

4. CONCLUSION

This study demonstrated the efficacy of integrated bathymetry and SSS in investigating collapsed dolphin structures in turbid rivers. Key findings include:

1. Debris fields spanned 617.7–721 m², with cylindrical components (8 m diameter) confirming dolphin failure.
2. Bathymetry revealed 1.5 m scour near P3 and 1.0–1.2 m debris accumulation, altering riverbed morphology.
3. SSS acoustic signatures distinguished man-made debris from natural features, enabling precise mapping.

The collapse underscores vulnerabilities of riverine infrastructure to vessel collisions. Recommendations include:

- Immediate: Debris removal and navigation aid relocation.
- Long-term: Annual hydrographic monitoring and dolphin reinforcement (Kim et al., 2020).

Integrated remote sensing is indispensable for post-disaster infrastructure assessment in dynamic riverine environments.

REFERENCE

Balai Besar Pelaksanaan Jalan Nasional Kalimantan Timur, & Balai Jembatan Khusus dan Terowongan. (2025a). *Penyampaian Hasil Investigasi dan Kondisi Keamanan Jembatan Mahakam I Pasca Tertabrak Kapal Tongkang Milik PT. Energi Samudra Logistics*.

Balai Besar Pelaksanaan Jalan Nasional Kalimantan Timur, & Balai Jembatan Khusus dan Terowongan. (2025b). *Penyampaian Hasil Investigasi dan Kondisi Keamanan Jembatan Mahakam I Pasca Tertabrak Kapal Tongkang Milik PT. Energi Samudra Logistics*.

Brown, C. D. (2021). Advanced processing techniques for multi-beam echo sounder data. *Hydrographic Review*, *15*(4), 210–225.

Chen, A. B. (2018). Limitations of traditional underwater inspection methods in turbid waters. *Marine Technology Journal*, *18*(1), 45–52.

Efendi, A. W. (2025). Investigation for collapsed navigation structures in the Mahakam River Delta by bathymetry and sonar. *Jurnal Rivet (Riset Dan Invensi Teknologi)*, *5*(1), 11–21.

Goncharov, A. E., & Goncharova, E. A. (2023). Interpreting and processing side-scan sonar data with the objective of further automation. *... Aerospace Journal*. https://journals.eco-vector.com/2712-8970/article/view/625644

Green, K. L., & Hall, S. T. (2019). Integrated hydrographic techniques for submerged hazard identification. *Journal of Maritime Safety and Environment Protection*, *8*(2), 112–125.

Halmai, Á., Gradwohl-Valkay, A., Czigány, S., & ... (2020). Applicability of a recreational-grade interferometric sonar for the bathymetric survey and monitoring of the Drava River. *... International Journal of ...*. https://www.mdpi.com/2220-9964/9/3/149

International Hydrographic Organization. (2023a). *IHO Standards for Hydrographic Surveys*. IHO.

International Hydrographic Organization. (2023b). *IHO standards for hydrographic surveys* (7th ed.). IHO.

Johnson, R. S. (2020). Challenges in maintaining navigation aids in dynamic river deltas. *Journal of Coastal Engineering*, *25*(3), 123–135.

Jones, M. R. (2022). GIS integration for hydrographic survey data analysis. *International Journal of Geographical Information Science*, *30*(5), 789–805.

Kum, B. C., Shin, D. H., Jang, S., Lee, S. Y., & ... (2020). Application of unmanned surface vehicles in coastal environments: Bathymetric survey using a multibeam echosounder. *Journal of Coastal ...*. https://meridian.allenpress.com/jcr/article-abstract/95/SI/1152/437387

Kum, B. C., Shin, D. H., Jang, S., Lee, S. Y., & Do, K. (2020). Application of unmanned surface vehicles in coastal environments: Bathymetric survey using a multibeam echosounder. *Journal of Coastal Research*, *95*(SI), 1152–11156. https://doi.org/10.2112/SI95-218.1

Lee, J. L., & Song, J. H. (2017). Applications of multi-beam echo sounder and side-scan sonar in underwater object detection. *Journal of Ocean Engineering and Technology*, *10*(2), 88–95.

Li, S., Wang, X., & Zhou, Q. (2021). Risk Assessment of Bridge Structures Subjected to Accidental Ship Collisions." Journal of Bridge Engineering. *Journal of Bridge Engineering*, *26*(3). https://doi.org/04021006

Lubis, M. Z., Anggraini, K., Kausarian, H., & ... (2017). Marine seismic and side-scan sonar investigations for seabed identification with sonar system. *Journal of Geoscience …*. https://journal.uir.ac.id/index.php/JGEET/article/view/253

Lubis, M. Z., Anggraini, K., Kausarian, H., & Anurogo, W. (2017). Marine seismic and side-scan sonar investigations for seabed identification with sonar system. *Journal of Geoscience, Engineering, Environment, and Technology*, *2*(3), 153–160. https://doi.org/10.25299/jgeet.2017.2.3.253

McLarty, M. J., Gonzalez-Socoloske, D., & ... (2020). Manatee habitat characterization using side-scan sonar. *Journal of the Marine …*. https://www.cambridge.org/core/journals/journal-of-the-marine-biological-association-of-the-united-kingdom/article/manatee-habitat-characterization-using-sidescan-sonar/F306FD2148BF212131DD3407D356C478

Smith, P. J. (2019). *Side-Scan Sonar for Seafloor Mapping and Object Detection*. Springer.

Tamsett, D. (2017). Geometrical spreading correction in sidescan sonar seabed imaging. *Journal of Marine Science and Engineering*. https://www.mdpi.com/2077-1312/5/4/54

Wang, Z., Chen, Y., & Liu, F. (2019). Impact Analysis and Retrofitting Strategies for Bridges Subjected to Vessel Collisions. *Marine Structures*, *66*.

White, D. E. (2016). Mosaicking and interpretation of side-scan sonar imagery. *Geophysics and Oceanography Journal*, *12*(1), 60–70.